

# Resonance Raman Spectrum of a ${}^2A_{1u}$ Ferryl Porphyrin $\pi$ -Cation Radical

Kazimierz Czarnecki,<sup>†</sup> L. M. Proniewicz,<sup>‡,§</sup> Hiroshi Fujii,<sup>\*,§</sup> and James R. Kincaid<sup>\*,†</sup>

Contribution from the Chemistry Department, Marquette University, Milwaukee, Wisconsin 53201-1881, Chemical Physics Division, Department of Chemistry, and Regional Laboratory of Physicochemical Analysis and Structural Research, Jagiellonian University, R. Ingardena Street 3, 30-060 Krakow, Poland, and Institute for Life Support Technology, Yamagata Technopolis Foundation, Kurumanomae 683, Numagi, Yamagata 990, Japan

Received December 4, 1995<sup>⊗</sup>

**Abstract:** Resonance Raman spectra are reported for the iron complex of tetramethyltetramesitylporphine (TMTMP) in its ferric, ferryl, and ferryl  $\pi$ -cation forms. For comparison, the spectra of the copper complex and its corresponding  $\pi$ -cation radical are included. Vibrational assignments have been made based on depolarization ratio measurements and isotopic frequency shifts associated with methine deuteration. The observed behavior of the  $\nu_2$  and  $\nu_{11}$  RR “marker bands”, which shift to higher frequency upon oxidation of the macrocycle, is consistent with previously reported NMR studies wherein these radicals were shown to have predominately  ${}^2A_{1u}$  ground states. The  $\nu(\text{Fe}=\text{O})$  stretching modes of the ferryl species (both five- and six-coordinate) and  $(\text{OFeTMTMP}^+)(\text{ClO}_4^-)$  are identified by their  ${}^{16}\text{O}/{}^{18}\text{O}$  isotope shifts. This is the first observation of the  $\nu(\text{Fe}=\text{O})$  mode for a  ${}^2A_{1u}$  type ferryl  $\pi$ -cation radical. Its frequency ( $833\text{ cm}^{-1}$ ) is virtually identical with that of the corresponding derivative of *meso*-tetramesitylporphyrin (TMP),  $(\text{O}=\text{FeTMP}^+)(\text{ClO}_4^-)$ , a  ${}^2A_{2u}$  radical, which exhibits its  $\nu(\text{Fe}=\text{O})$  mode at  $835\text{ cm}^{-1}$ . These data imply that the  $\nu(\text{Fe}=\text{O})$  modes of ferrylporphyrin  $\pi$ -cation radicals are rather insensitive to radical type ( ${}^2A_{1u}$  vs  ${}^2A_{2u}$ )—behavior which is surprisingly different from the previously observed sensitivity of the  $\nu(\text{V}=\text{O})$  modes of corresponding vanadylporphyrin  $\pi$ -cation radicals.

## Introduction

The key intermediate involved in the enzymatic cycles of a large number of oxidative heme enzymes such as peroxidases, catalases, and presumably cytochromes P450, is called compound I. These primary intermediates, which are two oxidizing equivalents higher than the resting state, are thought to contain an oxoiron(IV) porphyrin  $\pi$ -cation radical.<sup>1</sup> Depending on the symmetry of the highest occupied molecular orbital (HOMO), the ground electronic state of the heme  $\pi$ -cation radical can be assigned to one of two ( ${}^2A_{1u}$  or  ${}^2A_{2u}$ ) types<sup>2</sup> (*vide infra*). Their relative energies are dictated by several factors, such as position and type of substituents on the porphyrin macrocycle periphery or the nature of the axial ligand.<sup>3</sup>

Resonance Raman (RR) spectroscopy is a powerful tool in investigating the structure and bonding of these porphyrin

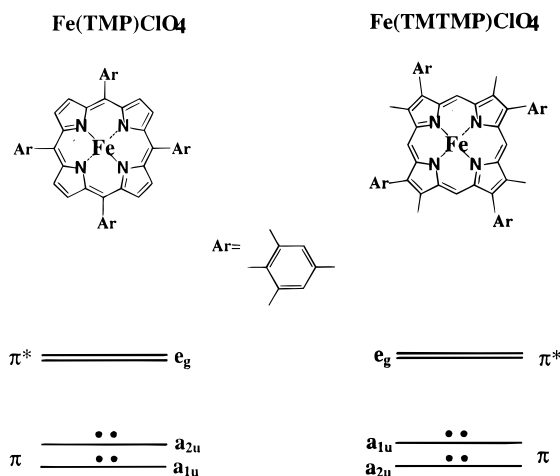


**Figure 1.** Structures of  $\text{Fe}^{\text{III}}(\text{TMP})\text{ClO}_4$  (TMP = 5,10,15,20-tetramesitylporphyrinato dianion) and  $\text{Fe}^{\text{III}}(\text{TMTMP})\text{ClO}_4$  (TMTMP = 2,7,12,17-tetramethyl-3,8,13,18-tetramesitylporphyrinato dianion) and their relative molecular orbital (HOMO-LUMO) energy levels.

$\pi$ -cation radicals.<sup>3a-d</sup> In principle, it is potentially able to provide direct documentation for the ferryl fragment *via* observation of the  $\text{Fe}=\text{O}$  stretching mode,  $\nu(\text{Fe}=\text{O})$ , and is effective in characterizing the nature of the electronic ground state of these radicals based on the frequencies of so-called RR “marker bands”.

$\text{Fe}^{\text{III}}(\text{TMTMP})\text{ClO}_4$  (TMTMP = 2,7,12,17-tetramethyl-3,8,13,18-tetramesitylporphyrinato dianion) (Figure 1) is the only iron porphyrin reported to form a stable  ${}^2A_{1u}$  ferryl porphyrin  $\pi$ -cation radical.<sup>4</sup> Like  $\text{Fe}^{\text{III}}(\text{TMP})\text{X}$  (where TMP = *meso*-tetramesitylporphyrinato dianion), it has four bulky-aryl substituents, but in this case the substituents are at the  $\beta$ -pyrrole

<sup>†</sup> Marquette University.

<sup>‡</sup> Jagiellonian University.

<sup>§</sup> Yamagata Technopolis Foundation.

<sup>⊗</sup> Abstract published in *Advance ACS Abstracts*, May 1, 1996.

(1) (a) Dunford, H. B. *Adv. Inorg. Biochem.* **1982**, 4, 41. (b) Frew, J. E.; Jones P. In *Advances in Inorganic and Bioinorganic Mechanism*; Academic Press: New York, 1984; Vol. 3, p 175. (c) Oertling W. A.; Kean, R. T.; Wever, R.; Babcock, G. T. *Inorg. Chem.* **1990**, 29, 2633.

(2) (a) Hanson, L. K.; Chang, C. K.; Davis, M. S.; Fajer, J. *J. Am. Chem. Soc.* **1981**, 103, 663. (b) Fujita, J.; Hanson, L. K.; Walker, F. A.; Fajer, J. *J. Am. Chem. Soc.* **1983**, 105, 3296. (c) Du, P.; Loew, G. H. *Biophys. J.* **1995**, 68, 69.

(3) (a) Czernuszewicz, R. S.; Macor, K. A.; Li, X.-Y.; Kincaid, J. R.; Spiro, G. T. *J. Am. Chem. Soc.* **1989**, 111, 3860. (b) Oertling, W. A.; Salehi, A.; Chang, C. K.; Babcock, G. T. *J. Phys. Chem.* **1989**, 93, 1311. (c) Macor, K. A.; Czernuszewicz, R. S.; Spiro, G. T. *Inorg. Chem.* **1990**, 29, 1996. (d) Kitagawa, T.; Mizutani, Y. *Coord. Chem. Rev.* **1994**, 135/136, 685. (e) Satoh, M.; Ohba, Y.; Yamauchi, S.; Iwazumi, M. *Inorg. Chem.* **1982**, 31, 298. (f) Keating, K. D.; DeRopp, J. S.; LaMar, G. N.; Balch, A. L.; Shaiu, F. Y.; Smith, K. M. *Inorg. Chem.* **1991**, 30, 3258. (g) Tan, H.; Simonis, U.; Shokhirev, N. V.; Walker, F. A. *J. Am. Chem. Soc.* **1994**, 116, 5784.

positions and the *meso* positions are unsubstituted. The function of these bulky substituents is to protect the active oxo ligand from the formation of the  $\mu$ -oxo dimer.<sup>5</sup> In addition, these substituents destabilize the  $a_{1u}$  molecular orbital to the extent that it becomes the HOMO (Figure 1). Therefore, upon oxidation of the porphyrin ring the first electron will be abstracted from the  $a_{1u}$  molecular orbital.<sup>3</sup> Furthermore, theoretical calculations<sup>6</sup> indicate that the unpaired electron density in the  $a_{1u}$  molecular orbital is localized to a greater extent at the  $\beta$ -pyrrole positions. The above theoretical predictions were confirmed by proton NMR measurements.<sup>4</sup>

The essential goal of this work is thus to provide a thorough RR study of this unique oxoiron(IV) compound. In order to achieve this goal we have measured the polarized RR spectra of  $\text{Fe}^{\text{III}}(\text{TMTMP})\text{ClO}_4$ , its *meso*-carbon-deuteriated analogue ( $-d_4$ ), the nonradical ferryl complexes (penta- and hexacoordinated), as well as the  $\pi$ -cation ferryl radical. In addition, we report here RR spectra of  $\text{Cu}^{\text{II}}(\text{TMTMP})$ ,  $\text{Cu}^{\text{II}}(\text{TMTMP}-d_4)$ , and their one-electron oxidation products, i.e.,  $\text{Cu}^{\text{II}}(\text{TMTMP}^{\bullet+})$  ( $\text{SbCl}_6^-$ ) ( $-h_4$  or  $-d_4$ , respectively). This rather complete data set permits assignment of the vibrational modes characteristic of the  $\pi$ -cation ferryl radical on the basis of  $-d_4$  isotopic frequency shifts and depolarization ratio measurements and thereby documents the (nonradical/ $\pi$ -cation radical) marker band frequency shifts. The results indicate that both  $\text{Cu}^{\text{II}}(\text{TMTMP})$  and  $\text{O}=\text{Fe}^{\text{IV}}(\text{TMTMP})$  form  ${}^2A_{1u}$  cation radicals upon oxidation, as previously inferred from NMR data.<sup>4</sup> More importantly, the present study documents, for the first time, the vibrational frequency of the  $\text{Fe}=\text{O}$  fragment of a  ${}^2A_{1u}$  ferrylporphyrin  $\pi$ -cation radical.

## Experimental Section

**Metalloporphyrin Complexes.** 2,7,12,17-Tetramethyl-3,8,13,18-tetramesitylporphyrin ( $\text{H}_2\text{TMTMP}$ ) was prepared by the literature method.<sup>7</sup> The *meso*-carbon-deuteriated analogue ( $\text{H}_2\text{TMTMP}-d_4$ ) was prepared from deuteriated 2-(hydroxymethyl)-3-mesityl-4-methylpyrrole which was obtained by the reduction of 2-(ethoxycarbonyl)-3-mesityl-4-methylpyrrole with  $\text{LiAlD}_4$  and acetic acid- $d_1$ . The deuterium NMR spectrum of the *meso*- $d_4$  porphyrin revealed 70% D-atom purity. Iron was inserted into the porphyrin by refluxing in a chloroform–acetic acid mixture (4:1) with ferrous chloride and sodium acetate.<sup>4b</sup> Copper insertion was achieved by refluxing the porphyrin in chloroform with copper acetate.<sup>8</sup> Copper complexes were purified by silica gel column chromatography and recrystallized from chloroform–methanol,<sup>9</sup> while the iron complexes were purified by column chromatography according to the following procedure. A glass column (about 30 cm  $\times$  1.5 cm), filled with toluene (Aldrich, HPLC grade), was slowly loaded (to  $\sim$ 25 cm line height) with dried alumina ( $\sim$ 400  $^\circ\text{C}$ ) (Aldrich, neutral, standard grade) and then with an  $\sim$ 2-cm layer of dried silica gel (J. T. Baker, 40–140 mesh) and equilibrated with 150 mL of toluene. A sample of the iron porphyrin (25 mg) was dissolved in  $\sim$ 2 mL of toluene and loaded onto the column. Development with toluene resulted in the elution of the metal-free ligand,  $\text{H}_2\text{TMTMP}$  (UV–vis in  $\text{CH}_2\text{Cl}_2$ : 402, 498, 530, 565, and 620 nm). Then, the heme was eluted with neat  $\text{CH}_2\text{Cl}_2$ . The main eluted heme fraction was concentrated by evaporation of solvent to  $\sim$ 10 mL and converted to the chloride form by stirring

overnight with a 0.1 M solution of aqueous hydrochloric acid.<sup>10</sup> The organic layer was separated and evaporated to dryness, and the resulting solid was recrystallized from toluene/heptane (UV–vis in  $\text{CH}_2\text{Cl}_2$ : 382, 508, 536, and 636 nm). The yield was 12 mg. The  $\text{Fe}^{\text{III}}(\text{TMTMP})\text{Cl}$  was converted to the perchlorate form by using the following procedure. A mixture of  $\text{Fe}^{\text{III}}(\text{TMTMP})\text{Cl}$  (12 mg, 13  $\mu\text{mol}$ ),  $\text{AgClO}_4$  (3 mg, 13  $\mu\text{mol}$ ), and toluene (5 mL) was boiled gently for 10 min, then filtered hot through a 0.45- $\mu\text{m}$  filter and concentrated to  $\sim$ 1.5–2.0 mL. Heptane ( $\sim$ 5 mL) was added dropwise and solution was allowed to set overnight to induce crystallization. Fine dark-violet crystals were collected by filtration, washed with heptane and dried under vacuum for  $\sim$ 5 h (UV–vis in  $\text{CH}_2\text{Cl}_2$ : 386, 500 (shoulder  $\sim$ 530) and 628 nm).  $\text{Fe}^{\text{II}}(\text{TMTMP})(\text{pip})_2$  was synthesized by a literature method<sup>11a</sup> and used as a starting material for the preparation of  $\text{O}=\text{Fe}(\text{TMTMP})$  according to the procedure of Balch *et al.*<sup>11b,c</sup>

**Solvents.** Dichloromethane ( $\text{CH}_2\text{Cl}_2$ , Aldrich, spectrophotometric grade) was purified<sup>12</sup> by shaking approximately 500 mL of spectrophotometric grade methylene chloride with 50–60 mL portions of concentrated  $\text{H}_2\text{SO}_4$  in a 1-L separatory funnel until the acid layer remained colorless.<sup>12</sup> The solvent was then washed 3 times with 100-mL portions of distilled water, passed through a  $\text{K}_2\text{CO}_3$  column, then predried over dried  $\text{CaCl}_2$ , distilled over  $\text{P}_2\text{O}_5$ , and directly passed through dried ( $>400$   $^\circ\text{C}$ ) neutral alumina column. *N,N*-Dimethylformamide (DMF, Aldrich, spectrophotometric grade) was dried with  $\text{MgSO}_4$  and then distilled under reduced pressure.<sup>12</sup> Toluene (Aldrich, spectrophotometric grade) was dried with sodium metal for 1 h and then distilled.

**Oxidants.** The gases  ${}^{16}\text{O}_2$  (Monsanto Research, 98%  ${}^{16}\text{O}_2$ ) and  ${}^{18}\text{O}_2$  (ICON, 98%  ${}^{18}\text{O}$  atom purity) were used without further purification. *m*-Chloroperoxybenzoic acid (*m*-CPBA( ${}^{16}\text{O}$ ), Aldrich, technical grade) was purified prior to use by washing its benzene solution with phosphate buffer of pH 7.5.<sup>13</sup> The benzene layer was dried over anhydrous  $\text{MgSO}_4$ , then filtered and carefully evaporated to dryness, and the solid was then recrystallized from  $\text{CH}_2\text{Cl}_2/\text{EtO}_2$ .<sup>14</sup> Iodometric titration<sup>15</sup> revealed 97% of active oxygen. Isotopically labeled *m*-CPBA( ${}^{18}\text{O}$ ) was synthesized using  ${}^{18}\text{O}_2$ , according to procedures described earlier.<sup>16</sup> Iodometric titration revealed 98% of active oxygen and Raman spectroscopy indicated 90% of  ${}^{18}\text{O}$ -labeled oxygen.

Ozone was produced by an electrical discharge (Tesla coil) in pure dioxygen.

Phenoxathiinium hexachloroantimonate ( $\text{Phx-SbCl}_6$ ) was prepared by the published procedure.<sup>17</sup>

**Oxidation Reactions.** The ferryl porphyrin  $\pi$ -cation radical in  $\text{CH}_2\text{Cl}_2$  was obtained by oxidation reactions with about a 4-fold excess of *m*-CPBA( ${}^{16}\text{O}$ ), and its ( ${}^{18}\text{O}$ ) analogue, at  $-80$   $^\circ\text{C}$  in a stirred, low-temperature cell according to the originally published procedure.<sup>4</sup> We note that use of only 4 equiv of *m*-CPBA prevents replacement of axially bound  $\text{ClO}_4^-$  and that oxidation of the ferric perchlorate species by ozone, using a procedure described elsewhere,<sup>18</sup> yields a spectrum identical to that obtained with 4 equiv of *m*-CPBA. The neutral ferryl porphyrin (six-coordinate, DMF adduct) was obtained by oxidation with *m*-CPBA( ${}^{16}\text{O}$ ) and its ( ${}^{18}\text{O}$ ) analogue at  $-44$   $^\circ\text{C}$  in a stirred, low-temperature cell according to the procedure of Gold *et al.*<sup>19</sup> The five-

(10) Cheng, R.-J.; Latos-Grazynski, L.; Balch, A. L. *Inorg. Chem.* **1982**, *21*, 2412.

(11) (a) Epstein, L. M.; Straub, D. K.; Maricondi, C. *Inorg. Chem.* **1967**, *6*, 1720. (b) Balch, A. L.; Chan, Y.-W.; Cheng, R.-J.; LaMar, G. N.; Latos-Grazynski, L.; Renner, M. W. *J. Am. Chem. Soc.* **1984**, *106*, 7779. (c) Chin, D.-H.; Balch, A. L.; LaMar, G. N. *J. Am. Chem. Soc.* **1980**, *102*, 1446.

(12) Perrin, D. P.; Armarego, W. L. F. In *Purification of Laboratory Chemicals*, 3rd ed.; Pergamon Press: Oxford, NY, 1988.

(13) Schwartz, N. N.; Blumberg, J. H. *J. Org. Chem.* **1964**, *29*, 1976.

(14) Bartolini, O.; Campestri, S.; DiFuria, F.; Modena, G. *J. Org. Chem.* **1987**, *52*, 5093.

(15) Traylor, T. G.; Miksztal, A. R. *J. Am. Chem. Soc.* **1987**, *109*, 2770.

(16) (a) Braun, G. *Organic Syntheses*; Wiley: New York, 1941; Collect. I, p 4131. (b) Rosenthal, I. *J. Labeled Compd.* **1976**, *12*, 317. (c) Johnson, R. A. *Tetrahedron Lett.* **1976**, *5*, 331.

(17) Gans, P.; Buisson, G.; Duèe, E.; Marchon, J.-C.; Erler, B. S.; Scholz, W. F.; Reed, C. A. *J. Am. Chem. Soc.* **1986**, *108*, 1223.

(18) Czarnecki, K.; Nimri, S.; Gross, Z.; Proniewicz, L. M.; Kincaid, J. R. *J. Am. Chem. Soc.* in press.

(19) Gold, A.; Jayoraj, K.; Doppelt, P.; Weiss, R.; Chottard, G.; Bill, E.; Ding, X.; Trautwein, A. X. *J. Am. Chem. Soc.* **1988**, *110*, 5756.

(4) (a) Fujii, H. *J. Am. Chem. Soc.* **1993**, *115*, 4641. (b) Fujii, H.; Ichikawa, K. *Inorg. Chem.* **1992**, *31*, 1110.

(5) (a) Dunford, H. B.; Stillman, J. S. *Coord. Chem. Rev.* **1976**, *19*, 187. (b) Dunford, H. B. *Adv. Inorg. Biochem.* **1982**, *4*, 41. (c) McMurry, T. J.; Groves, J. T. In *Cytochrome P-450: Structure, Mechanism, and Biochemistry*; Ortiz de Montellano, P. R., Ed.; Plenum: New York, 1986; Chapter I.

(6) (a) Gouterman, M. In *The Porphyrins*; Dolphin, D., Ed.; Academic Press: New York, 1978; Vol. III. (b) Spangler, D.; Maggiora, G. M.; Shipman, L. L.; Christofferson, R. E. *J. Am. Chem. Soc.* **1977**, *99*, 7478.

(7) Ono, N.; Kawamura, H.; Bougauchi, M.; Maruyama, K. *Tetrahedron* **1990**, *46*, 7483.

(8) Adler, A. D.; Longo, F. R.; Varadi, V. *Inorg. Synth.* **1976**, *16*, 213.

(9) Fujii, H. *Inorg. Chem.* **1993**, *32*, 875.

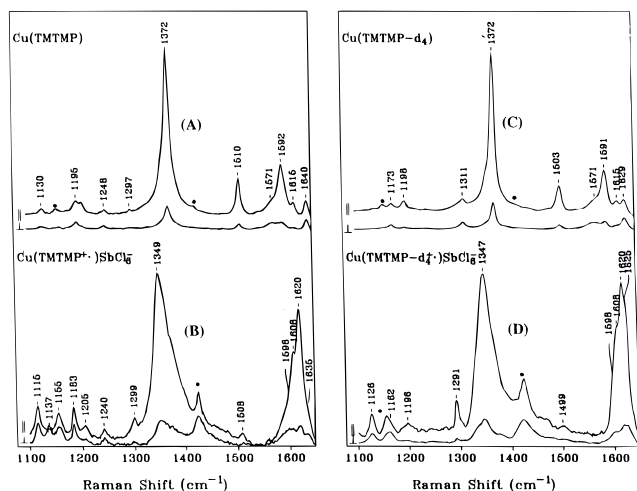


**Figure 2.** The high-frequency polarized resonance Raman spectra of  $\text{Cu}^{\text{II}}(\text{TMTMP})\text{ClO}_4$  complexes measured in  $\text{CH}_2\text{Cl}_2$  at room temperature with excitation at 406.7 nm (spinning NMR tube,  $135^\circ$  scattering geometry): (A)  $\text{Cu}^{\text{II}}(\text{TMTMP})$ ; (B)  $\text{Cu}^{\text{II}}(\text{TMTMP}^+)(\text{SbCl}_6^-)$ ; (C)  $\text{Cu}^{\text{II}}(\text{TMTMP}-d_4)$ ; (D)  $\text{Cu}^{\text{II}}(\text{TMTMP}-d_4^+)(\text{SbCl}_6^-)$ . Bands marked with asterisks are due to solvent bands.

coordinate ferryl porphyrin was obtained *via* an autooxidation reaction of the dioxygen adduct at  $-70^\circ\text{C}$ , using a procedure reported by Balch *et al.*<sup>11b,c</sup>

$\text{Cu}^{\text{II}}(\text{TMTMP})$  and its *meso*- $d_4$  analogue were oxidized with  $\text{Phx-SbCl}_6$  in the following way:  $\text{Cu}^{\text{II}}(\text{TMTMP})$  was dissolved in  $\text{CH}_2\text{Cl}_2$  and stirred for 15 min. Then  $\text{Phx-SbCl}_6$  (1.1 equiv) was added slowly and the suspension was stirred for another hour. After filtration, hexane was added dropwise to the filtrate and the solution was left overnight. The resultant crystals were filtered, washed with hexane–dichloromethane mixture (4:1), and dried under vacuum.

**Spectroscopic Measurements.** Low-temperature RR measurements were performed using a stirred Dewar cell with a cylindrical lens setup to minimize possible thermal or photodecomposition<sup>20</sup> of the observed species. Room temperature measurements were performed using a standard spinning cell technique with a  $135^\circ$  back-scattering geometry. Spectra were acquired with a single monochromator (SPEX Model 1269) fitted with a CCD detector (Princeton Instrument) and notch filter (Kaiser Optical System, Ann Arbor, MI). The frequencies were calibrated by using known frequencies of toluene and fenchone and are accurate to within  $\pm 1\text{ cm}^{-1}$ . No digital smoothing was performed on any of the spectra. The 406.7-nm line of the Coherent Model Innova 100-K3 Krypton ion laser (with the power 5 to 10 mW at the sample) was used as an excitation source. In the case of the oxidized compounds, RR spectra were acquired sequentially in separate files and summed. Those later files, which began to exhibit new features ascribable to thermal or photochemical degradation, were not included in the summation. Also, in the case of the ferryl  $\pi$ -cation samples (which are notoriously subject to photodegradation),<sup>3d</sup> RR spectra were acquired at several different incident laser powers in an attempt to ensure that none of the observed spectral features were contributed by photoproducts. Optical spectra (UV–vis) were measured in a low-temperature Dewar cell using a Hewlett-Packard 8452A diode array spectrometer.

## Results and Discussion

**1.  $\text{Cu}^{\text{II}}(\text{TMTMP})$  and Its Cation Radical.** Figure 2 compares RR spectra of  $\text{Cu}^{\text{II}}(\text{TMTMP})$ , its  $-d_4$  analogue, and their corresponding porphyrin  $\pi$ -cation radicals, all obtained with 406.7-nm excitation. The RR spectra presented in traces A and C exhibit spectral patterns quite similar to those observed for other pyrrole  $\beta$ -carbon-substituted metalloporphyrins, such as  $\text{M}(\text{OEP})$  complexes ( $\text{M}$  = metal;  $\text{OEP}$  = octaethylporphyrinato

dianion).<sup>3a,b</sup> Since the excitation line is within the Soret absorption band the most intense features observed in these spectra are associated with totally symmetric (polarized) modes; i.e., A-term scattering is responsible for their enhancement.<sup>21</sup> The most intense skeletal modes observed in the high-frequency region are the following:  $\nu_2$  [ $\nu(\text{C}_\beta\text{--C}_\beta)$ ],  $\nu_3$  [ $\nu(\text{C}_\alpha\text{--C}_\beta)_{\text{sym}}$ ], and  $\nu_4$  [ $\nu(\text{pyr, half ring})_{\text{sym}}$ ].<sup>3a,b,22</sup> Also, owing to the Jahn–Teller effect,<sup>21,23</sup> depolarized bands assigned to  $\nu_{10}$  [ $\nu(\text{C}_\alpha\text{--C}_\beta)_{\text{asym}}$ ] and  $\nu_{11}$  [ $\nu(\text{C}_\beta\text{--C}_\beta)$ ]<sup>21,23</sup> are observed with appreciable intensity.

Three polarized bands at 1372, 1510, and 1592  $\text{cm}^{-1}$  are observed in trace A. In addition, the 1510- $\text{cm}^{-1}$  band downshifts (7  $\text{cm}^{-1}$ ) upon deuteration at the *meso*-carbon positions. Thus, this band is assigned to the  $\nu_3$  mode by comparison with reported deuterium shifts for  $\text{M}(\text{OEP})$  complexes.<sup>3a–c,21,23</sup> In addition to the typical OEP-type macrocycle vibrations, a phenyl mode, located at 1615  $\text{cm}^{-1}$ , is observed in Figure 2.

Upon oxidation of  $\text{Cu}^{\text{II}}(\text{TMTMP})$  or its  $-d_4$  analogue with  $\text{Phx-SbCl}_6$  the porphyrin  $\pi$ -cation radicals are formed. The RR spectra of these species (traces B and D) are much weaker than those exhibited by the parent metalloporphyrins (traces A and C), i.e., upon comparing intensities of the vibrations of the complexes with those of the solvent, which are marked with asterisks. This intensity decrease is typically observed upon radical cation formation.<sup>3d</sup> The RR spectra presented in traces B and D are also dominated by polarized bands at ca. 1349 and 1620  $\text{cm}^{-1}$ . Based on their insensitivity to deuterium isotopic substitution and depolarization ratios, these bands are readily assigned to the  $\nu_4$  and  $\nu_2$  modes, respectively. They experience 23- and 28- $\text{cm}^{-1}$  downshifts relative to neutral  $\text{Cu}(\text{TMTMP})$ . Careful examination of traces B and D reveals the polarized  $\nu_3$  mode at 1508  $\text{cm}^{-1}$  (trace B) which shifts to 1499  $\text{cm}^{-1}$  in the case of the  $-d_4$  analogue (trace D). The depolarized  $\nu_{10}$  and  $\nu_{11}$  bands can be seen more clearly in the spectra measured with perpendicular polarization. Thus,  $\nu_{10}$  is observed at 1635  $\text{cm}^{-1}$  (trace B) and exhibits a 10- $\text{cm}^{-1}$  downshift upon deuterium substitution. The  $\nu_{11}$  mode is seen at 1598  $\text{cm}^{-1}$ . The RR pattern and the observed deuterium isotopic shifts of these five marker bands agree very well with those observed for other  $\text{M}(\text{OEP}^+)$  complexes.<sup>3a–c</sup> The observed frequencies are listed in Table 1 together with mode assignments.

The  $\nu_2$  and  $\nu_{11}$  modes are the most reliable as markers to distinguish between  $^2\text{A}_{1u}$  and  $^2\text{A}_{2u}$  types of metalloporphyrin  $\pi$ -cation radicals.<sup>3a–d</sup> These modes involve mainly stretching vibrations of the  $\text{C}_\beta\text{--C}_\beta$  bond,  $\nu(\text{C}_\beta\text{--C}_\beta)$ .<sup>3a,b</sup> The  $a_{1u}$  molecular orbital is antibonding with respect to the  $\text{C}_\beta\text{--C}_\beta$  bond, while the  $a_{2u}$  is bonding.<sup>6</sup> Thus, oxidation of the porphyrin macrocycle in the case where the  $a_{1u}$  molecular orbital is the HOMO strengthens the  $\text{C}_\beta\text{--C}_\beta$  bond and gives rise to the observed shifts to higher frequency for the  $\nu_2$  and  $\nu_{11}$  modes. Conversely, formation of a  $^2\text{A}_{2u}$  metalloporphyrin  $\pi$ -cation radical leads to the opposite result, i.e., weakening of the  $\text{C}_\beta\text{--C}_\beta$  bond and concomitant downshifts of these modes. Thus, the RR data presented here confirm that  $\text{Cu}^{\text{II}}(\text{TMTMP}^+)$  has a  $^2\text{A}_{1u}$  ground state, which is as expected for radicals of metalloporphyrins

(21) Spiro, T. G.; Czernuszewicz, R. S. *Meth. Enzymol.* **1995**, 246, 416.

(22) (a) Li, X.-Y.; Czernuszewicz, R. S.; Kincaid, J. R.; Stein, P.; Spiro, T. G. *J. Phys. Chem.* **1990**, 94, 47. (b) Li, X. Y. Ph.D. Dissertation, Princeton University, 1988.

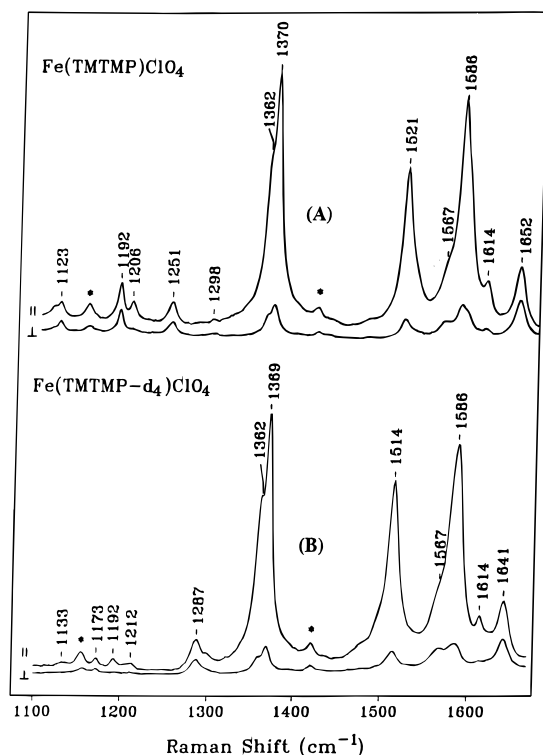
(23) Shelnutt, J. A.; Cheung, L. D.; Cheng, C. C.; Yu, N. T.; Felton, R. H. *J. Chem. Phys.* **1977**, 66, 3387.

(20) (a) Kincaid, J. R.; Schneider, A. J.; Paeng, K.-J. *J. Am. Chem. Soc.* **1989**, 111, 735. (b) Proniewicz, L. M.; Paeng, I. R.; Nakamoto, K. *J. Am. Chem. Soc.* **1991**, 113, 3294.

**Table 1.** Resonance Raman Frequencies ( $\text{cm}^{-1}$ ) for  $\text{Cu}^{\text{II}}(\text{TMTMP})$ ,  $\text{Cu}^{\text{II}}(\text{TMTMP}^{\bullet+})$ ,  $\text{Fe}^{\text{III}}(\text{TMTMP})\text{ClO}_4$ ,  $\text{O}=\text{Fe}^{\text{IV}}(\text{TMTMP})$ ,  $\text{O}=\text{Fe}^{\text{IV}}(\text{TMTMP}^{\bullet+})\text{ClO}_4$ , and  $\text{M}(\text{OEP}^{\bullet+})$  Complexes

mode	$\text{Cu}(\text{TMTMP})$ ( $\Delta d_4$ )	$\text{Cu}(\text{TMTMP}^{\bullet+})$ ( $\Delta d_4, \Delta \text{ox}$ )	$\text{Fe}^{\text{III}}(\text{TMTMP})\text{ClO}_4$ ( $\Delta d_4$ )	$\text{O}=\text{Fe}^{\text{IV}}(\text{TMTMP})$ ( $\Delta d_4$ )	$\text{M}(\text{OEP}^{\bullet+})^a$ ( $\Delta \text{ox}$ )	$\text{O}=\text{Fe}^{\text{IV}}(\text{TMTMP}^{\bullet+})\text{ClO}_4$ ( $\Delta \text{ox}$ )
$\nu_{10}$ (dp)	1640 (−11)	1635 (−10, −5)	1652 (−11)	1631 (−7)	−7 to −10	
$\nu_{\text{ph}}$ (p)	1615 (0)	1608 (0, 7)	1614 (0)	1614 (0)		
$\nu_2$ (p)	1592 (−1)	1620 (0, 28)	1586 (0)	1593 (0)	21 to 23	1623 (30)
$\nu_{11}$ (dp)	1571 (0)	1598 (0, 27)	1567 (0)	1578 (−2)	33	1614 (36)
$\nu_3$ (p)	1510 (−7)	1508 (−9, −2)	1521 (−7)	1511 (−7)	−2 to −8	1499 (−11)
$\nu_4$ (p)	1372 (0)	1349 (−2, −23)	1370 (−1)	1374 (0)	−5 to −17	1363 (−10)
			1362 (0)			
$\nu(\text{Fe}=\text{O})$				845 (0)		834 (−11)
$\nu(\text{Fe}=\text{O})$				809 (0)		798 (−11)

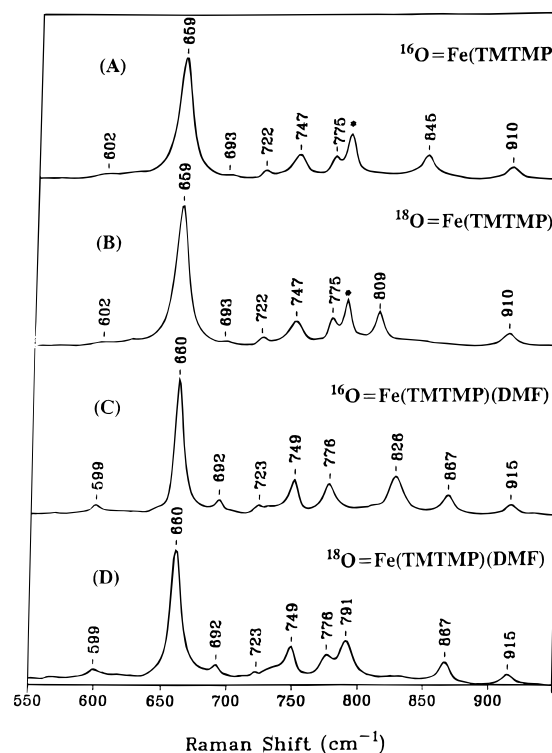
<sup>a</sup> See refs 3a and 3b. For mode descriptions see ref 22.  $\Delta d_4$  and  $\Delta \text{ox}$  = frequency shifts ( $\text{cm}^{-1}$ ) upon *meso*- $d_4$  isotopic substitution and  $\pi$ -cation porphyrin radical formation, respectively.

**Figure 3.** The high-frequency polarized resonance Raman spectra of  $\text{Fe}^{\text{III}}(\text{TMTMP})\text{ClO}_4$  (trace A) and  $\text{Fe}^{\text{III}}(\text{TMTMP-}d_4)\text{ClO}_4$  (trace B) measured in  $\text{CH}_2\text{Cl}_2$  at room temperature with excitation at 406.7 nm.

bearing eight  $\beta$ -pyrrole substituents (in the absence of strong donor ligands).<sup>2,3,6</sup>

**2. Ferric and Ferryl Derivatives.** Figure 3 shows the polarized RR spectra of  $\text{Fe}^{\text{III}}(\text{TMTMP})\text{ClO}_4$  (trace A) and  $\text{Fe}^{\text{III}}(\text{TMTMP-}d_4)\text{ClO}_4$  (trace B) in the high-frequency region, both obtained in  $\text{CH}_2\text{Cl}_2$  with 406.7-nm excitation. The main marker modes ( $\nu_2$ ,  $\nu_3$ ,  $\nu_4$ ,  $\nu_{10}$ , and  $\nu_{11}$ ), as for the  $\text{Cu}^{\text{II}}(\text{TMTMP})$  complex, can be assigned on the basis of deuterium shifts, observed depolarization ratios, and comparison with the literature data reported for corresponding  $\text{M}(\text{OEP})$  complexes.<sup>3a-c,22</sup> Assignments of these key marker bands are presented in Table 1.

Figure 4 shows the low-frequency RR spectra of five-coordinate  $\text{O}=\text{Fe}^{\text{IV}}(\text{TMTMP})$  and six-coordinate  $\text{O}=\text{Fe}^{\text{IV}}(\text{TMTMP}(\text{DMF}))$ . Trace A presents the RR spectrum of  $^{16}\text{O}=\text{Fe}^{\text{IV}}(\text{TMTMP})$  measured in toluene (i.e., noncoordinating solvent) at  $-70^\circ\text{C}$  with excitation at 406.7 nm. Upon  $^{16}\text{O}/^{18}\text{O}$  isotopic substitution only one RR band shifts: from 845 (trace A) to 809  $\text{cm}^{-1}$  (trace B). These bands are therefore assigned to the  $\nu(\text{Fe}-^{16}\text{O})$  and  $\nu(\text{Fe}-^{18}\text{O})$ , respectively, of  $^{16}\text{O}=\text{Fe}^{\text{IV}}(\text{TMP})$  and its  $^{18}\text{O}$  analogue. The observed isotopic shift is in good

**Figure 4.** The low-frequency resonance Raman spectra of (A)  $^{16}\text{O}=\text{Fe}^{\text{IV}}(\text{TMTMP})$  and (B)  $^{18}\text{O}=\text{Fe}^{\text{IV}}(\text{TMTMP})$  in toluene at  $-70^\circ\text{C}$  and (C)  $^{16}\text{O}=\text{Fe}^{\text{IV}}(\text{TMTMP})(\text{DMF})$  and (D)  $^{18}\text{O}=\text{Fe}^{\text{IV}}(\text{TMTMP})(\text{DMF})$  in DMF at  $-44^\circ\text{C}$  with excitation at 406.7 nm. Bands marked with asterisks are due to solvent bands.

agreement with that expected ( $38\text{ cm}^{-1}$ ) for a harmonic diatomic  $\text{Fe}=\text{O}$  oscillator. Similar RR results have been reported by several groups<sup>24</sup> for other ferrylporphyrins in toluene at low temperature, where  $\nu(\text{Fe}-\text{O})$  was observed near  $845\text{ cm}^{-1}$ .

The  $\text{O}^{2-}$  axial ligand donates both  $\sigma$  and  $\pi$  electrons (fully occupied p orbitals) to the  $\text{Fe}(\text{IV})$  ion.<sup>1c,3d,25</sup> The  $\sigma$  bond is thus formed by interaction of the  $d_z$  (Fe) orbital with the  $p_z$  (O) orbital. Since  $\text{Fe}(\text{IV})$  has a  $d^4$  electronic configuration, the two valence electrons are accommodated in the  $d_{xy}$  orbital (in plane, nonbonding) and the remaining two electrons are involved in formation of  $\pi$  bonds. Thus, the sixth ligand, trans to the oxo atom, also donates  $\sigma$  and  $\pi$  electron density, weakening the  $\text{Fe}=\text{O}$

(24) (a) Hashimoto, S.; Tatsuno, Y.; Kitagawa, T. *Proceedings of the 10th International Conference on Raman Spectroscopy*; Peticolas, W. L., Hudson, B., Eds.; Eugene, OR, 1986; p 1.28. (b) Su, Y. O.; Czernuszewicz, R. S.; Miller, L. A.; Spiro, T. G. *J. Am. Chem. Soc.* **1988**, *110*, 4150. (c) Paeng, I. R.; Shiwaku, H.; Nakamoto, K. *J. Am. Chem. Soc.* **1988**, *110*, 1995. (d) Mizutani, Y.; Hashimoto, S.; Tatsuno, Y.; Kitagawa, T. *J. Am. Chem. Soc.* **1990**, *112*, 6809.

(25) Proniewicz, L. M.; Bajdor, K.; Nakamoto, K. *J. Phys. Chem.* **1986**, *90*, 1760.

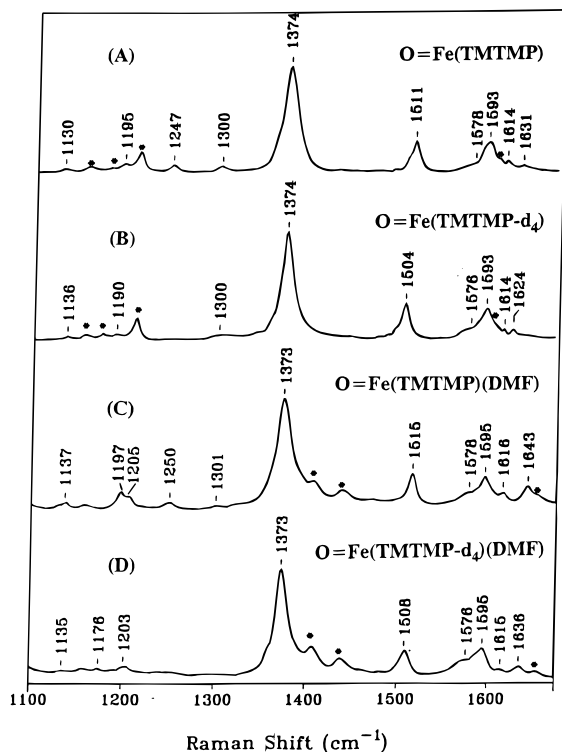


**Figure 5.** The high-frequency resonance Raman spectra of (A)  $\text{O}=\text{Fe}^{\text{IV}}(\text{TMTMP})$  and (B)  $\text{O}=\text{Fe}^{\text{IV}}(\text{TMTMP-}d_4)$  in toluene at  $-70^\circ\text{C}$  and (C)  $\text{O}=\text{Fe}^{\text{IV}}(\text{TMTMP})(\text{DMF})$  and (D)  $\text{O}=\text{Fe}^{\text{IV}}(\text{TMTMP-}d_4)(\text{DMF})$  in DMF at  $-44^\circ\text{C}$  with excitation at 406.7 nm. Bands marked with asterisks are due to solvent bands.

bond. As a result the  $\nu(\text{Fe}-\text{O})$  mode will downshift. This is illustrated in traces C and D of Figure 4, where  $\nu(\text{Fe}-^{16}\text{O})$  and  $\nu(\text{Fe}-^{18}\text{O})$  are downshifted, in response to DMF ligation to 826 and  $791\text{ cm}^{-1}$ , respectively. These observed  $\nu(\text{Fe}-\text{O})$  frequencies agree very well with those reported for other six-coordinate neutral ferryl derivatives.<sup>17,26</sup> Also in this case, the isotopic frequency shift is in agreement with that theoretically expected.

Comparison of the high-frequency spectra (Figure 5) of  $\text{O}=\text{Fe}^{\text{IV}}(\text{TMTMP})$  and its  $-d_4$  analogue reveals two deuterium isotope sensitive modes at  $1511$  ( $\Delta\nu_{d_4} = -7\text{ cm}^{-1}$ ) and  $1631\text{ cm}^{-1}$  ( $\Delta\nu_{d_4} = -7\text{ cm}^{-1}$ ). These bands are reasonably assigned to the  $\nu_3$  and  $\nu_{10}$  modes, respectively. The intense mode at  $1374\text{ cm}^{-1}$  is not sensitive to  $\text{meso-}d_4$  isotopic substitution and is assigned to the  $\nu_4$  mode. The  $\nu_2$  and  $\nu_{11}$  modes are observed at  $1593$  and  $1578\text{ cm}^{-1}$ . The observed frequencies are listed in Table 1 together with mode assignments.

In traces C and D of Figure 5 the high-frequency RR spectra of six-coordinate  $\text{O}=\text{Fe}^{\text{IV}}(\text{TMTMP})(\text{DMF})$  and its  $\text{meso-}d_4$  analogue, respectively, are presented. Trace C exhibits bands at  $1373$ ,  $1515$ , and  $1595\text{ cm}^{-1}$ , which are polarized (omitted in the figure for clarity). The band at  $1515\text{ cm}^{-1}$  shifts down by  $7\text{ cm}^{-1}$  upon  $\text{meso-}d_4$  deuteration, while the other two do not shift. Thus, these bands are assigned to the  $\nu_4$ ,  $\nu_3$ , and  $\nu_2$  modes, respectively. The bands at  $1578$  and  $1643\text{ cm}^{-1}$  in trace C are depolarized. While the former is not sensitive to the  $\text{meso-}d_4$  isotopic substitution, the latter shows a  $7\text{-cm}^{-1}$  downshift (trace D). These are assigned to the  $\nu_{11}$  and  $\nu_{10}$  modes, respectively.

**3. Ferryl  $\pi$ -Cation Porphyrin Radical.** The high-frequency polarized RR spectra of  $\text{O}=\text{Fe}(\text{TMTMP}^+)\text{ClO}_4$  and its  $\text{meso-}d_4$  analogue measured in  $\text{CH}_2\text{Cl}_2$  at  $-80^\circ\text{C}$  with

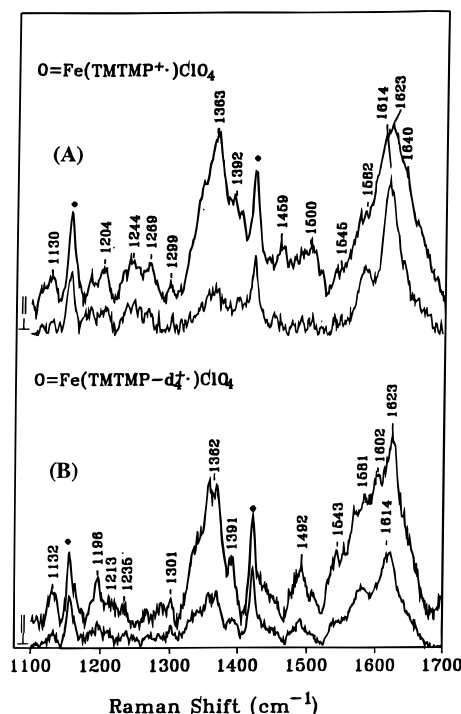


**Figure 6.** The high-frequency resonance Raman spectra of (A)  $\text{O}=\text{Fe}^{\text{IV}}(\text{TMTMP}^+)\text{ClO}_4$  and (B)  $\text{O}=\text{Fe}^{\text{IV}}(\text{TMTMP-}d_4^+)\text{ClO}_4$  obtained with parallel and perpendicular polarization. Samples were measured in  $\text{CH}_2\text{Cl}_2$  at  $-80^\circ\text{C}$  with excitation at 406.7 nm. Bands marked with asterisks are due to solvent bands.

excitation at 406.7 nm are shown in Figure 6. Here, it is necessary to point out that, owing to the instability of the observed  $\pi$ -cation radical species, it was difficult to acquire polarized spectra; i.e., they are not of high quality. Nevertheless, these spectra reveal, in the region of the  $\nu_3$  mode, a polarized band at  $1499\text{ cm}^{-1}$  (trace A), which is shifted to  $1492\text{ cm}^{-1}$  upon  $\text{meso-}d_4$  deuteration (trace B). Since the observed isotopic shift and polarization properties fit very well to the shift of the  $\nu_3$  mode observed for  $\text{Fe}^{\text{III}}(\text{TMTMP})\text{ClO}_4$  and the ferryl derivatives, this band is assigned to this mode. Since the high-frequency spectra of observed porphyrin  $\pi$ -cation radicals in regions of other marker modes consist of envelopes of several modes it is not possible to definitively identify  $\nu_4$ ,  $\nu_2$ ,  $\nu_{11}$ , and  $\nu_{10}$ .

However, the band at  $1363\text{ cm}^{-1}$  is a polarized mode and thus it is a good candidate for  $\nu_4$ . Note that this band is downshifted by  $11\text{ cm}^{-1}$  from the  $\nu_4$  mode of  $\text{O}=\text{Fe}^{\text{IV}}(\text{TMTMP})$  (see Figure 5). The spectra given in Figure 6 show that there is a strong polarized mode centered near  $1623\text{ cm}^{-1}$  and a depolarized mode occurring at  $\sim 1614\text{ cm}^{-1}$ . The polarized component can be reasonably attributed to  $\nu_2$  since it shows no  $d_4$  shift. As is clear in the figure, the depolarized mode exhibits an insignificant deuterium shift and therefore the most reasonable assignment for the  $1614\text{-cm}^{-1}$  feature is to  $\nu_{11}$ , the  $\nu_{10}$  mode apparently being too weak to be observed. These assignments are summarized in Table 1. Note that data in parentheses represent shifts calculated by comparing  $(\text{OFeTMTMP}^+)\text{ClO}_4$  with the five-coordinate  $\text{O}=\text{Fe}^{\text{IV}}\text{TMTMP}$ .

Figure 7 shows the low-frequency RR spectra of  $\text{O}=\text{Fe}^{\text{IV}}(\text{TMTMP}^+)\text{ClO}_4$  and its  $\text{meso-}d_4$  deuterated analogue in  $\text{CH}_2\text{Cl}_2$  (temperature  $-80^\circ\text{C}$ , excitation at 406.7 nm), both obtained by oxidation with  $m\text{-CPBA}(^{16}\text{O})$  (about four equivalences) or its  $(^{18}\text{O})$  isotopic analogue. As can be seen, traces A and C reveal a mode at ca.  $833\text{ cm}^{-1}$ , which is shifted to  $798\text{ cm}^{-1}$  upon oxygen isotopic substitution (traces B and D). This mode

(26) (a) Schappacher, M.; Chottard, G.; Weiss, R. *J. Chem. Soc., Chem. Commun.* **1986**, 93. (b) Kean, R. T.; Oertling, W. A.; Babcock, G. T. *J. Am. Chem. Soc.* **1987**, *109*, 2185. (c) Chen, S. M.; Su, Y. O. *J. Chem. Soc., Chem. Commun.* **1990**, 491.

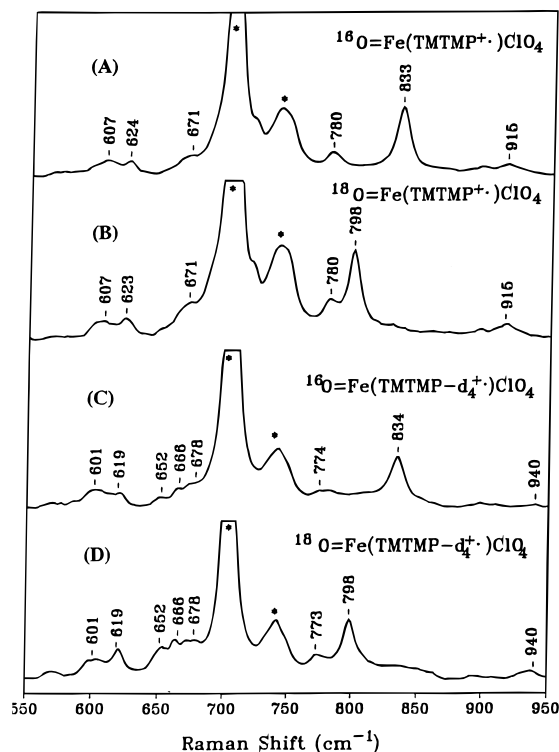


**Figure 7.** The low-frequency resonance Raman spectra of (A)  ${}^{16}\text{O}=\text{Fe}^{\text{IV}}(\text{TMTMP}^{\bullet+})\text{ClO}_4$ , (B)  ${}^{18}\text{O}=\text{Fe}^{\text{IV}}(\text{TMTMP}^{\bullet+})\text{ClO}_4$ , (C)  ${}^{16}\text{O}=\text{Fe}^{\text{IV}}(\text{TMTMP}-d_4^{\bullet+})\text{ClO}_4$ , and (D)  ${}^{18}\text{O}=\text{Fe}^{\text{IV}}(\text{TMTMP}-d_4^{\bullet+})\text{ClO}_4$ . Samples were measured in  $\text{CH}_2\text{Cl}_2$  at  $-80^\circ\text{C}$  with excitation at 406.7 nm. Bands marked with asterisks are due to solvent bands.

is therefore assigned to the iron(IV)–oxo stretching frequency of the  $\text{O}=\text{Fe}^{\text{IV}}(\text{TMTMP}^{\bullet+})\text{ClO}_4$ .

In the present study it is observed that the  $\nu(\text{Fe}=\text{O})$  of  $\text{O}=\text{Fe}(\text{TMTMP}^{\bullet+})(\text{ClO}_4^-)$  occurs at  $833\text{ cm}^{-1}$ , while that for the five-coordinate (neutral) ferryl derivative,  $\text{O}=\text{Fe}(\text{TMTMP})$ , occurs at  $845\text{ cm}^{-1}$ . We note here that quite similar values are observed for the corresponding derivatives of TMP; i.e., the  $\nu(\text{Fe}=\text{O})$  for  $\text{OFe}(\text{TMP})$  occurs at around  $843\text{ cm}^{-1}$ ,<sup>24</sup> and for  $\text{OFe}(\text{TMP}^{\bullet+})(\text{ClO}_4^-)$  it occurs at  $835\text{ cm}^{-1}$ .<sup>18</sup> While the

observed shift upon oxidation of either (neutral) ferryl complex reflects both an oxidation-induced component and a response to addition of an (albeit weak) axial ligand ( $\text{ClO}_4^-$ ), to the extent that coordination induced shifts are presumably similar for these two iron porphyrins, the oxidation-induced shifts are also comparable. That is, apparently the oxidation-induced shift of the  $\text{Fe}=\text{O}$  fragment is insensitive to the nature ( $a_{1u}$  vs  $a_{2u}$ ) of the HOMO.

To our knowledge, this is the first observation of the  $\nu(\text{Fe}=\text{O})$  mode of an authentic  ${}^2A_{1u}$  ferryl porphyrin  $\pi$ -cation radical model compound and provides the first opportunity to make a direct comparison of the influence of radical type ( ${}^2A_{1u}$  vs  ${}^2A_{2u}$ ) on the  $\text{Fe}=\text{O}$  fragment. The only previous studies relevant to the present comparison are the reports of the RR spectra of the corresponding vanadyl complexes of OEP, TPP, and TMP.<sup>3c,27</sup> There it was reported that the behavior of the  $\nu(\text{V}=\text{O})$  mode is dependent on the nature of the HOMO ( $a_{1u}$  vs  $a_{2u}$ ). Thus, for  $\text{OV}(\text{OEP})$ , which forms an  ${}^2A_{1u}$  radical upon oxidation of the macrocycle,  $\nu(\text{V}=\text{O})$  shifts up (to  $1002\text{ cm}^{-1}$ ) relative to its value ( $987\text{ cm}^{-1}$ ) for the neutral complex.<sup>27</sup> On the other hand, the  $\nu(\text{V}=\text{O})$  for an  ${}^2A_{2u}$  radical (i.e.,  $\text{OV}(\text{TPP}^{\bullet+})$ ) shifts down (to  $982\text{ cm}^{-1}$ ) relative to its value ( $998\text{ cm}^{-1}$ ) for the neutral  $\text{OV}(\text{TPP})$ .<sup>27</sup>

In the present work, in attempting to compare the influence of radical type on observed  $\nu(\text{Fe}=\text{O})$  frequencies, care was taken to ensure constancy of the trans-axial ligand (i.e.,  $\text{ClO}_4^-$ ). To the extent that axial ligation differences did not exist in the comparison of the vanadyl analogues,<sup>27</sup> there appears to be a real difference in the systems (ferryl vs vanadyl) with respect to the influence of radical type on the  $\nu(\text{M}=\text{O})$  frequencies.

**Acknowledgment.** This work was supported by a grant (to JRK) from the National Institutes of Health (DK35153). JRK also thanks the Wehr Foundation for partial support of this work. Partial support of LMP by Grant 2P 303 060 05 from the Polish Committee for Scientific Research (KBN) is gratefully acknowledged.

JA954044X

(27) Macor, K. A.; Czernuszewicz, R. S.; Spiro, T. G. *Inorg. Chem.* **1990**, 29, 1996.